

The use of ilmenite as oxygen-carrier in a 500 W_{th} Chemical Looping Coal Combustion unit

A. Cuadrat, A. Abad^{*}, F. García-Labiano, P. Gayán, L. F. de Diego, J. Adánez

Instituto de Carboquímica (CSIC), Dept. of Energy & Environment, Miguel Luesma Castán 4,
50018-Zaragoza, Spain

^{*} Corresponding author: Tel: (+34) 976 733 977. Fax: (+34) 976 733 318. E-mail address:
abad@icb.csic.es (A. Abad)

Abstract

Chemical-Looping Combustion, CLC, is a promising technology to capture CO₂ at low cost in fossil-fuelled power plants. In CLC the oxygen from air is transferred to the fuel by a solid oxygen-carrier that circulates between two interconnected fluidized-bed reactors: the fuel- and the air-reactor.

This work studies the CLC technology in a 500 W_{th} facility fuelled with bituminous coal with ilmenite as oxygen-carrier. The effect of temperature and coal particle size on coal conversion and combustion efficiency was assessed. Char gasification and combustion of both gasification products and volatile matter were evaluated. At higher temperatures, gasification and combustion reactions are promoted. Carbon capture and combustion efficiencies grow

with the temperature, with faster increase at temperatures higher than 910°C. The outgoing unburnt gases come from volatile matter that was not fully oxidized by ilmenite. Little CH₄ was measured and there were neither hydrocarbons heavier than CH₄ nor tars in the fuel-reactor outlet. At 870°C the char conversion was 15% and reached 82% at 950°C. The combustion efficiency in the fuel-reactor increased from 70% at 870°C to 95% at 950°C. The results show that ilmenite has good behavior as oxygen-carrier and that optimizing CLC with coal can lead to energy production with high CO₂ capture.

Keywords: Chemical-Looping Combustion, Oxygen-carrier, Ilmenite, CO₂ capture, Coal.

1. Introduction

Anthropogenic carbon dioxide emissions, which mainly come from the combustion of fossil fuels for power generation, transport and industry, significantly contribute to global warming (IPCC, 2007). Therefore, there is a need to decrease CO₂ emissions in order to stabilize its concentration in the atmosphere. Since fossil fuels are still the dominant energy source worldwide and the transition to more sustainable energy system is a slow process, CO₂ capture and sequestration (CCS) has been proposed as an important option to reduce CO₂ emissions from power production. Current CCS technologies, available or under development, have the disadvantage of high costs and energy penalties, associated mainly to the CO₂ capture process, recovering the gas from flue streams.

Chemical-Looping Combustion (CLC) is one of the most promising technologies to carry out CO₂ capture in power plants at a low cost (IPCC, 2005; Eide et al., 2005; Kerr, 2005). In this process the CO₂ separation from the other flue gas components is inherent to the process and thus no energy is expended for the capture. The CLC concept is based on the transfer of oxygen from the combustion air to fuel by means of an oxygen-carrier in the form of a metal

oxide, which takes place in two separate reactors. In CLC systems, the conventional combustion reaction is replaced by two successive reactions forming a chemical loop. The solids circulate between two interconnected reactors, the fuel-reactor and the air-reactor. In the fuel-reactor, the metal oxide reacts with the gaseous fuel to produce CO₂ and H₂O. Pure CO₂, ready to compression and storage, will be readily recovered by condensing the steam. It could be advantageous if the CLC process could be adapted to the use of solid fuels. In the Chemical Looping Combustion with coal the solid fuel is directly introduced to the fuel-reactor, where is converted to CO₂ and H₂O by the oxygen transferred from the oxygen-carrier. In this case the gasification of the solid fuel is carried out in the fuel-reactor simultaneously as the oxygen-carrier reacts with the products of the fuel devolatilization and gasification (Adánez et al., 2011). In this process the fuel-reactor is fluidized by a gasifying agent, e.g., H₂O or CO₂, as proposed by Cao et al. (Cao et al., 2006). Thereby, the solid fuel gasification takes place in the same reactor first according to reactions (1-3) and the resulting gases and volatiles are oxidized through reduction of the oxidized oxygen-carrier, Me_xO_y, by means of reaction (4). The oxygen-carrier reduced in the fuel-reactor, Me_xO_{y-1}, is later led to the air-reactor where it is oxidized with air by reaction (5), and it is ready to start a new cycle. The net chemical reaction as well as the heat involved in the global process is the same as for normal fuel gas combustion.

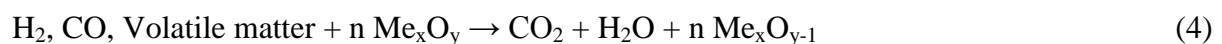


Figure 1 shows the simplified reactor scheme of the CLC process with direct introduction of solid fuels, which counts with the air- and fuel- reactors, the circulating oxygen-carrier. As the gasification process is expected to be the limiting step in the fuel-reactor, the solids stream going out from the fuel-reactor can contain certain fraction of unconverted char. Thus, a carbon stripper step is proposed to separate char from the oxygen-carrier (Cao et al., 2006; Berguerand and Lyngfelt, 2008a).

For direct CLC with solid fuels, there are 3 particular aspects to be taken into account: (1) to reach high combustion efficiencies it is necessary to have good contact between the oxygen-carrier particles and the volatile matter and gasification products, (2) the system must be optimized to get maximum ash separation and minimum carrier extraction, since part of the carrier will be removed together with the draining of ashes present in the solid fuel, and (3) the carbon stripper should be optimized for the carbon separation. Otherwise, the CO₂ capture efficiency will be reduced because of CO₂ exiting together with the depleted air stream.

The research on CLC with solid fuels concludes that gasification is probably the rate-limiting step (Leion et al., 2008; Bidwe et al., 2010). Linderholm et al. studied the gasification rates for a wide variety of coal chars, showing the feasibility of using the CLC technology with different type of coals with the appropriate design modifications or high efficiency carbon stripper implementation (Linderholm et al., 2010). Cuadrat et al. (Cuadrat et al., 2011a) studied the fuel-reactor performance regarding the gasification rate and later reaction of ilmenite with the gasification products in batch fluidized bed with South African coal char feed. They calculated an optimal range of solids inventory in the fuel-reactor of 500-1000 kg/MW_{th} to get char conversions as high as 90-95%, which is feasible and adequate for this technology.

A key factor for the CLC technology development is the selection of the oxygen-carrier. Solid particles based on Fe, Ni and Cu have been extensively investigated as feasible oxygen-

carriers to be used in CLC systems, as reviewed by Adánez et al. (Adánez et al., 2011) Suitable oxygen-carriers for a CLC process must have high reactivity during reduction and oxidation, high attrition resistance and agglomeration absence.

To evaluate the performance of CLC with solid fuels, several works have been done in continuously operated coal fuelled CLC prototypes. Shen et al. (Shen et al., 2009a; 2009b; 2010) used a synthetic NiO/Al₂O₃ oxygen-carrier in two continuous facilities with different particle recirculation system design of thermal power of 10 kW_{th} and 1 kW_{th}. Although they had some CO and CH₄ in the fuel-reactor product gas, high coal conversions to CO₂ were reached. For the 10 kW_{th} rig, they found that coal gasification controlled the CO and CH₄ concentrations in the fuel-reactor product gas, as well as the carbon capture efficiency. They obtained a carbon conversion efficiency of 92.8% at a fuel-reactor temperature of 970°C. The 1 kW_{th} rig had an improved external particle recirculation configuration that reduced the char particles escaping to the air-reactor. A CO₂ capture of 95% at 985°C was then reached. Although no major operational problems occurred and good results were obtained, the use of NiO based oxygen-carriers at industrial-scale presents some disadvantages due to its higher cost and environmental issues.

Low cost of the material is rather desirable for its use with coal, as a partial loss together with the coal ashes is predictable when removing them from the reactor to avoid their accumulation in the system. Recently, interest on the use of CaSO₄ as oxygen-carrier has been showed by several research groups. For instance, CaSO₄ from natural anhydrite is a low cost material with much higher oxygen transport capacity than other proposed materials but lower reactivity with reducing gases (H₂, CO and CH₄) (Wang and Anthony, 2008; Song et al., 2008).

Furthermore, there are some studies on the suitability of using some minerals as iron ore, ilmenite, manganese ore or waste materials coming from steel industry and alumina

production. Leion et al. (Leion et al., 2009) and Fossdal et al. (Fossdal et al., 2010) analyzed the behavior of several iron and manganese ores, as well as iron and manganese industrial products, during repeated redox cycles at fluidizing conditions using syngas or methane as fuel gases. Regarding the reactivity, Fossdal et al. (Fossdal et al., 2010) found a Mn ore as the most promising for CLC applications. However, Leion et al. concluded that manganese ores showed poor mechanical stability and poor fluidizing properties making them unsuitable as oxygen-carriers (Leion et al., 2009). They found adequate materials based on manganese and iron industrial products. In addition, iron based minerals, exhibited high reactivity with mixtures of H₂ and CO being suitable for both solid fuelled CLC and syngas combustion. An Australian natural mineral based in hematite as oxygen-carrier was used by Gu et al. (Gu et al., 2010). They successfully tested the CLC process during 30 hours in a 1 kW_{th} facility with coal as fuel. Combustion efficiencies of 82- 87% were obtained at a fuel-reactor temperature of 950°C. Besides, the adequate behavior of an iron waste material as oxygen-carrier with respect to gas combustion was proved in a continuous 500 W_{th} CLC prototype by Ortiz et al. (Ortiz et al., 2010) using a simulated PSA off-gas stream, methane and syngas as fuel. Among all these low cost materials, ilmenite is a natural mineral which is promising for its large scale industrial use as oxygen-carrier with solid fuels. It is mainly composed of FeTiO₃ (FeO·TiO₂), where iron oxide is the active phase that behaves as the oxygen-carrier.

Performance of ilmenite has been proved to be acceptable as oxygen-carrier for CLC in recent studies made at different scales. Reactivity of ilmenite in a batch fluidized bed for solid fuels combustion was studied by Leion et al. (Leion et al., 2008a) Ilmenite gave high conversion of CO and H₂ but moderate conversion of CH₄. Fresh ilmenite reacts slowly, but there is a gain in reactivity in reduction as well as in oxidation with the number of cycles (Adánez et al., 2010), and eventually reactivities as high as for a synthetic Fe₂O₃-based oxygen-carrier were reached (Leion et al., 2008b). The reaction kinetics of ilmenite for both reduction and

oxidation reactions taking place in the CLC process was studied by Abad et al. (Abad et al., 2011). This activation occurred for H₂, CO as well as CH₄ as fuel gases, and was faster if ilmenite had been previously calcined. The initial oxygen transport capacity was measured to be 4% and it decreased with the number of cycles. In continuous operation with natural gas and syngas as fuel, a Norwegian ilmenite was tested in a 120 kW CLC facility by Pröll et al. (Pröll et al., 2009). Although some conditions needed optimization, reasonable fuel conversion for CO and H₂ at 950°C was obtained. Furthermore, syngas was combusted at 900°C in a CLC dual fluidized bed system using an Australian ilmenite by Bidwe et al. resulting in a steady-state conversion of circa 90% (Bidwe et al., 2010).

For ilmenite as oxygen-carrier, the feasibility of the CLC process in the bigger scale and continuous operation was proved in a 10 kW_{th} chemical-looping combustor using South African coal and petroleum coke as solid fuels by Berguerand et al. (Berguerand and Lyngfelt, 2008a; 2008b). This rig counts with a carbon stripper to increase the residence time of char particles in the fuel-reactor. However, due to the feeding system, part of the volatile matter exits the system without getting in contact with the oxygen-carrier bed and therefore the analysis was only made to the gas conversion of the gasification products, i.e., H₂ and CO. The combustion of a Mexican petroleum coke using ilmenite as oxygen-carrier was tested during 26 hours (Berguerand and Lyngfelt, 2009a). A CO₂ capture within the range 65-82% was obtained, which are rather low values mainly because the fuel has low reactivity. The performance of this rig could be improved by increasing the residence time of the particles in the fuel-reactor to get higher CO₂ capture and by increasing the separation efficiency of the cyclone after the fuel-reactor. The solid fuel conversion was 65-70%, whereas the incomplete gas conversion resulted into the presence of unconverted gases, i.e. CH₄, CO, H₂ and H₂S, in the fuel-reactor outlet stream that demanded 29-30% of the total oxygen needed to fully burn coal to H₂O and CO₂. The gas conversion could be improved by a polishing step after the

fuel-reactor, or through a fuel-reactor design that got better contact between the gases released by the fuel and the oxygen-carrier bed. When a more reactive coal was used, it was confirmed that high carbon capture efficiencies can be obtained: 82-96% (Berguerand and Lyngfelt, 2009a). Although in all tests there was some fraction of unconverted gases, i.e. H₂ and CO, the importance of using high temperatures in this process to get both high fuel and gas conversions was proven, and the oxygen demand at a fuel-reactor temperature of 1000°C was as low as 5-7% (Berguerand and Lyngfelt, 2009b). Furthermore, the effect that the mean residence time of char particles given by a determined solids circulation flow-rate has on the char conversion was assessed (Markström et al., 2010).

On the whole, all studies to date confirm the feasibility of the CLC technology with solid fuels and that ilmenite appears to be a suitable material to be used for solid fuel combustion in a CLC system, considering its chemical and physical properties and low cost. Nevertheless, the good behavior of the fuel-reactor is fundamental for the reliability of a CLC system. On the one hand, it will determine the gas losses obtained at the exit of the reactor and the possible necessity to take additional actions, as to recirculate the unburned gases, e.g. CO, H₂ or CH₄, after removing H₂O and CO₂ from the flue gas, or to add a final gas polishing step by O₂ addition. On the other hand, the gasification rate will affect the char concentration in the bed and the carbon stripper performance.

The aim of this work was to investigate the capability of ilmenite to process coal as fuel in a coal fuelled CLC reactor, when ilmenite is continuously circulated between the fuel- and air-reactor and coal is continuously fed to the fuel-reactor. The conversion of gasifying products and volatile matter to CO₂ and H₂O by reaction with ilmenite was studied in a 500 W_{th} unit, besides the gasification of char in the fuel-reactor. A Colombian bituminous coal was used as fuel. The experiments were carried out at 820-950°C in the fuel-reactor, and the fluidizing gas was pure steam, which also acts as gasifying agent. The effect of fuel-reactor temperature and

coal particle size on the extent of gasification in the fuel-reactor and oxygen polishing requirements was investigated. Special attention was done in the relevance of gasifying products and volatiles in the oxygen demand. Furthermore, the evolution of chemical and physical properties of ilmenite particles with the time in continuous operation was also evaluated. The results obtained are analyzed and discussed in order to be useful for the scale-up of the CLC with solids fuel process.

2. Experimental

2.1. Ilmenite and coal

The oxygen-carrier used in this work is an iron titanium oxide called ilmenite, which is extracted from a natural ore and provided by the Norwegian company Titania A/S and received in its reduced form FeTiO_3 . The ilmenite used was pre-calcined at 950°C . The pre-oxidation was carried out to get ilmenite to its most oxidized state and improve properties and initial reaction rates (Adánez et al., 2010; Leion et al., 2008b). Moreover, a pre-oxidation of ilmenite was also beneficial in order to avoid defluidization problems (Pröll et al., 2009). The same type of ilmenite has been already used in several studies in continuous testing (Bidwe et al., 2010; Berguerand and Lyngfelt, 2008a; 2008b; 2009a; 2009b; Cuadrat et al., 2011c). The oxidized species present in ilmenite are Fe_2TiO_5 , Fe_2O_3 and TiO_2 , and its reduced state for the CLC technology is mainly composed of FeTiO_3 , Fe_3O_4 and TiO_2 . The initial oxygen transport capacity was measured to be 4.0%. Table 1 shows the compositions of both fresh and calcined ilmenite. The true density of ilmenite particles was 3980 kg/m^3 . The particle size used was +150-300 μm . More details about the composition, physical properties and reactivity of ilmenite particles can be found elsewhere (Adánez et al., 2010, Abad et al., 2011).

The fuel used was a bituminous Colombian coal “El Cerrejón”. The coal was subjected to a thermal pre-treatment for pre-oxidation in order to reduce its swelling properties. Thus, coal

was placed in trays in layers of about 3 mm height and exposed to heating at 180°C in air atmosphere for 28 hours. The use of pre-treated coal avoids the pipe clogging and coal particles agglomeration showed when fresh coal was used. Ultimate and proximate analyses of the fresh and pre-treated coal are shown in Table 2. The pre-oxidation causes an increase in oxygen content and a decrease in the heating value. The density of coal particles was 1600 kg/m³. Three different coal particle sizes were used: +74-125, +125-200 and +200-300 μm.

Char of the used coal was produced and fed as fuel in the CLC system in order to evaluate separately the combustion of char and of volatile matter. Thus, part of the pre-treated coal was devolatilized by heating it up to 900°C in a batch fluidized bed reactor, keeping the solids permanently in bubbling bed conditions fluidized with N₂ in inert atmosphere. The ultimate analysis of the resulting char is shown in Table 3. The char particle size was +125-200 μm.

2.2. Oxygen-carrier characterization

Various samples of ilmenite were taken to evaluate the evolution and change of the particles properties during the continuous performance. The textural properties of the oxygen-carrier samples were determined by Hg intrusion in a Quantachrome PoreMaster 33; solid density was measured by a He Micromeritics AccuPyc II 1340 picnometer.

A thermogravimetric analyzer (TGA) was used for the determination of the reactivity and activation extent of ilmenite by means of its reaction rate in reduction and oxidation of every extracted sample. The TGA was also used to measure the oxygen transport capacity of the samples. The thermogravimetric analyzer is a CI Electronics type. More information about this set-up can be found elsewhere (Adánez et al., 2004). The experiments were performed at 900°C with a 5% H₂+40% H₂O mixture, and afterwards to oxidation conditions in air. The reductions were done with a reducing gas with a H₂O:H₂ ratio of 8:1 to ensure that the final

oxygen-carrier reduced species are FeTiO_3 and Fe_3O_4 . The reaction rates of the samples extracted during the continuous testing were compared to the initial calcined ilmenite and a fully activated sample.

2.3. 500 W_{th} coal fuelled CLC reactor

In this work, the CLC technology with a Colombian bituminous coal was investigated in the ICB-CSIC-s1 continuous rig using ilmenite as oxygen-carrier. A schematic view of the experiment facility is shown in Figure 2. The CLC system was basically composed of two interconnected fluidized-bed reactors, the fuel-reactor (FR) (1) and the air-reactor (AR) (3), joined by a loop seal (2), a riser (4) for solids transport from the air- to the fuel-reactor, a cyclone to recover the entrained solids (5) and a solids valve (7) to control the flow rate of solids fed to the fuel-reactor. The temperatures in the different sectors of the plant can be set, as it is heated up by various furnaces (10), i.e. in the air-reactor and bottom bed and freeboard of the fuel-reactor.

The fuel-reactor consisted of a bubbling fluidized bed with 5 cm of inner diameter and 20 cm bed height. Coal (8) is fed by a screw feeder at the bottom of the bed above the fuel-reactor distributor plate in order to maximize the time that volatile matter is in contact with the bed material. The screw feeder (9) has two steps: the first one with variable speed to control the coal flow rate, and the second has high rotating velocity to avoid coal pyrolysis inside the screw. A small N_2 flow is fed in the beginning of the screw to avoid possible volatile reverse flow or entrance of steam. The maximum thermal power capacity of the unit was 500 W_{th} for the Colombian coal used in this work. In the fuel-reactor the oxygen-carrier is reduced by the volatile matter and gasification products of coal, where H_2 and CO are the main components. The fuel-reactor is fluidized by steam, which acts also as a gasifying agent. The solid fuel devolatilization proceeds in the fuel-reactor first and the resulting gases and gasification

products are oxidized through reduction of the oxidized ilmenite. Reduced oxygen-carrier particles overflowed into the air-reactor through a U-shaped fluidized bed loop seal with an inner diameter of 5 cm, to avoid gas mixing between fuel and air. Since this rig has no carbon stripper, unconverted char from the fuel-reactor goes to the air-reactor and is fully burnt there, releasing the CO₂ that is measured in the air-reactor. The implementation of a carbon stripper would decrease the CO₂ flow in the air-reactor and thereby the carbon capture efficiency would increase. However, the absence of a carbon stripper facilitates the interpretation of the effect of these operational conditions on the results obtained.

The oxidation of the carrier took place in the air-reactor, consisting of a bubbling FB fluidized with air with 8 cm of inner diameter and 10 cm bed height, and followed by a riser. Secondary air was introduced at the top of the bubbling bed to help particle entrainment. N₂ and unreacted O₂ left the air-reactor and went through a high-efficiency cyclone and a filter before the stack. The oxidized solid particles recovered by the cyclone were sent to a solids reservoir, setting the oxygen-carrier ready to start a new cycle. These particles act as a loop seal avoiding the leakage of gas between the fuel-reactor and riser. Previous testing in the ICB-CSIC-s1 continuous rig confirmed that there was no gas leakage between reactors and that the pressure balance was adequate. The regenerated oxygen-carrier particles returned to the fuel-reactor by gravity from the solids reservoir through a solids valve which controlled the flow rates of solids entering the fuel-reactor. The solid valve consist of a hole which can be partially closed by a sliding sheet. A diverting solids valve located below the cyclone allowed the measurement of the solids flow rates at any time. The total ilmenite bed mass in the system was 3.5 kg and the solids bed mass in the fuel-reactor was 0.8 kg ilmenite, as the solids level in the fuel-reactor is fixed and the exceeding overflows and heads for the air-reactor.

In the fuel-reactor a steam flow of 180 L_N/h was introduced (corresponding to a velocity of 0.11 m/s at 900°C) and in the air-reactor the total stream of primary plus secondary air flow was 2500 L_N/h (corresponding to a velocity of 0.6 m/s at 900°C). The circulation flow rate was measured and controlled to be about 3.5 kg/h and the coal flow was about 42 g/h, corresponding to a thermal power of 255 W_{th}. That is, the solids hold-up in the fuel-reactor was 1764 kg/MW_{th}.

During operation, temperatures in the bed and freeboard of the fuel-reactor, air-reactor bed and riser were monitored as well as the pressure drops in important locations of the system, such as the fuel-reactor bed, the air-reactor bed and the loop seal. Because of its small size, the system is not auto-thermal and is heated up with various ovens to get independent temperature control of the air-reactor, fuel-reactor, and fuel-reactor freeboard. The temperature in the air-reactor was maintained at around 950°C and the fuel-reactor temperature was varied from 820°C to 950°C. The fuel-reactor freeboard is kept constant at about 900°C in all the experiments. Different experiments were carried out varying the temperature and using different particle size of coal. 40 different stable conditions were reached with ilmenite as bed material: in 30 of them coal was fed and 10 with char. One further experiment was done with coal as fuel, but silica sand as inert bed material. At least every condition was maintained stable during 30 minutes. A total of 35 hours of continuous operation feeding fuel and 42 hours of continuous fluidization were made.

CO, CO₂, H₂, CH₄, and O₂ were continuously analyzed in the exit streams from the fuel-reactor and from the air-reactor. Nondispersive infrared (NDIR) analyzers (Maihak S710/UNOR) were used for CO, CO₂, and CH₄ concentration determination; a paramagnetic analyzer (Maihak S710/OXOR-P) was used for O₂ concentration determination; and a thermal conductivity detector (Maihak S710/THERMOR) was used for H₂ concentration determination. All data were collected by means of a data logger connected to a computer. In

some selected experiments the tar amount present in fuel-reactor product gases was determined following the tar protocol (Simell et al., 2000). Collection of moisture and tar was performed in a series of 8 impinger bottles by absorption in isopropanol and later cooling in external baths. Two different cooling baths were used. The first was an ice bath, where the first 2 impingers were located. The first was empty and the second contains isopropanol. These impingers recover the majority of moisture and aromatic tar compounds (styrene, indene, benzene, etc.) and light Polycyclic aromatic hydrocarbons (PAHs), mainly naphthalene. The second bath contains 6 impingers at -18°C . Several gaseous samples from the fuel-reactor stream were also taken in bags in order to measure the components through gas chromatography analysis.

3. Data evaluation

The evaluation of the fuel-reactor performance is carried out by the analysis of two main parameters: the carbon capture and the combustion efficiency. The oxygen demand is also calculated in order to know the oxygen requirements in the oxygen polishing step, if required. The purpose of the data evaluation is to assess the performance of the process in the different experiments done, using the measured values of the variables.

The efficiencies that indicate the performance of the process are defined as follows. The carbon capture efficiency, η_{CC} , is the fraction of the carbon introduced that is converted to gas in the fuel-reactor. As it will be later explained, as carbon containing species in the fuel-reactor product gas only CH_4 , CO and CO_2 were taken into account, as the measured tars and hydrocarbons heavier than CH_4 were negligible. The carbon measured in the gases coming from the fuel-reactor and the air-reactor is less than the carbon present in the introduced coal, because there is elutriation of char. However, in case of an industrial plant the possible elutriated char will be collected in a cyclone and reintroduced in the fuel-reactor. The

elutriated char flow was calculated as the difference between the fed coal carbon and the measured carbon in the fuel-reactor and air-reactor outlet gas flows. Thus, only the effective coal fed was considered to evaluate the performance of the plant. The carbon of the effective coal is the sum of all carbon containing species measured in the outlet streams of both fuel- and air-reactor. The calculations for the technology assessment were therefore done following these considerations. Thus, the carbon capture efficiency was calculated as:

$$\eta_{CC} = \frac{F_{CO_2,FR} + F_{CO,FR} + F_{CH_4,FR}}{F_{CO_2,FR} + F_{CO,FR} + F_{CH_4,FR} + F_{CO_2,AR}} \quad (6)$$

$F_{CH_4,FR}$, $F_{H_2,FR}$ and $F_{CO,FR}$ being the flows in the fuel-reactor of CH_4 , H_2 and CO . These flows were calculated from the CH_4 , H_2 and CO concentrations at the fuel-reactor exit which were on-line analyzed. The carbon of the unreacted char flowing towards the air-reactor is the CO_2 gas flow in the air-reactor, $F_{CO_2,AR}$.

The gas flows of every gas were calculated by multiplying the corresponding gas fraction and the outlet gas flow, i.e. F_{FR} in the case of the fuel-reactor, and F_{AR} for the air-reactor. The dry basis product gas flow, F_{FR} , was calculated by using the N_2 flow $F_{N_2,FR}$ that is introduced in the fuel-reactor coming from the Loop Seal. Preliminary results showed that about 65% of the N_2 introduced to fluidize the Loop Seal went to the fuel-reactor and the rest to the air-reactor. The outlet air-reactor gas flow, F_{AR} , was calculated though the introduced N_2 , $F_{N_2,AR}$, which is sum of the N_2 present in the air introduced in the air-reactor and the N_2 coming from the Loop Seal.

$$F_{FR} = \frac{F_{N_2,FR}}{1 - (y_{CH_4,FR} + y_{CO_2,FR} + y_{CO,FR} + y_{H_2,FR})} \quad (7)$$

$$F_{AR} = \frac{F_{N_2,AR}}{1-(y_{CO_2,AR} + y_{O_2,AR})} \quad (8)$$

$y_{CH_4,FR}$, $y_{CO_2,FR}$, $y_{CO,FR}$ and $y_{H_2,FR}$ are the dry basis fractions in the fuel-reactor product gas of CH₄, CO₂, CO and H₂, respectively. $y_{O_2,AR}$, $y_{CO_2,AR}$ are the fractions in the air-reactor outlet flow of O₂ and CO₂ respectively. The char conversion, X_{char} , is defined as the fraction of carbon in the effective char fed to the fuel-reactor which is released to the fuel-reactor outgoing gas stream:

$$X_{char} = \frac{C_{char,FR}}{C_{char,eff}} = \frac{F_{CO_2,FR} + F_{CO,FR} + F_{CH_4,FR} - C_{vol}}{F_{CO_2,FR} + F_{CO,FR} + F_{CH_4,FR} + F_{CO_2,AR} - C_{vol}} \quad (9)$$

The char converted in the fuel-reactor, $C_{char,FR}$, was calculated as difference of the carbon in gases in the fuel-reactor outgoing flow, and the carbon flow coming from the volatile matter, C_{vol} . The carbon content of the volatiles is directly calculated using the elementary and proximate analyses of both the coal used and char. $C_{char,eff}$ is the carbon contained in the introduced effective char and was calculated as the carbon flow in the effective coal minus the carbon flow coming from the volatile matter.

The combustion efficiency, η_{comb} , is a measure of gas conversion and represents the extent of oxidation of volatiles and gasification products by the oxygen-carrier. The combustion efficiency in the fuel-reactor is calculated as the fraction of the oxygen demanded by the volatile matter and gasification products that is supplied by the oxygen-carrier in the fuel-reactor. It is therefore dependent on the reaction rate of ilmenite with the gaseous fuels and on the amount of gases generated. The oxygen supplied by ilmenite in the fuel-reactor is calculated through the oxygen containing species in the fuel-reactor product gas. The sum of

volatile matter and gasified char is calculated as the effective coal introduced minus the char flowing towards the air-reactor, $F_{CO_2,AR}$. For a carbon stripper with 100% separation efficiency, no CO_2 would go to the air-reactor and the here defined combustion efficiency would correspond to the efficiency of combustion of the effective coal. Therefore, the combustion efficiency was calculated as:

$$\eta_{comb} = \frac{0.5 \cdot (F_{H_2O,FR\ out} - F_{H_2O,in}) + F_{CO_2,FR} + 0.5 \cdot F_{CO,FR} - 0.5 \cdot O_{coal,eff}}{O_{2\ demand\ coal,eff} - F_{CO_2,AR}} \quad (10)$$

$F_{H_2O,FR}$, $F_{CO_2,FR}$ and $F_{CO,FR}$ being, respectively, the fuel-reactor outlet flows of water, CO_2 and CO. $O_{coal,eff}$ is the flow of oxygen contained in the effective coal introduced. $O_{2\ demand\ coal,eff}$ or the oxygen demand of the effective coal flow is the oxygen flow needed to burn the fuel completely and is calculated with the volatile matter in the coal feed and the effective char flow.

An total oxygen demand for the fuel-reactor gases, Ω_T , was defined, as the fraction of oxygen lacking to achieve a complete combustion of the fuel-reactor product gas in comparison to the oxygen demand of the effective introduced coal, $O_{2\ demand\ coal,eff}$. This parameter is the most adequate to evaluate the performance of the combustion process in this facility, since it is the demand of the coal actually involved in the conversion process in the fuel-reactor.

$$\Omega_T = \frac{O_{2\ demand\ gases\ FR}}{O_{2\ demand\ coal,eff}} = \frac{2 \cdot F_{CH_4,FR} + 0.5 \cdot F_{H_2,FR} + 0.5 \cdot F_{CO,FR}}{O_{2\ demand\ coal,eff}} \quad (11)$$

The residence time of char and ilmenite particles were calculated assuming perfect mixing of ilmenite in the fuel reactor. Assuming that char and ash present in the bed are low, the mean residence time of ilmenite, $t_{m,ilm}$, is calculated by equation (12).

$$t_{m,ilm} = \frac{m_{ilm,FR}}{F_{ilm}} \quad (12)$$

$m_{ilm,FR}$ being the fuel-reactor bed mass or solid hold-up in the fuel-reactor, and F_{ilm} the solids circulation rate. The mean residence time for ilmenite was calculated to be about 14 minutes in all experiments.

The elutriation of char particles affect to the residence time of these particles in the reactor. The residence time of ilmenite and char would be the same, but since there is char elutriation, the mean residence time of char, $t_{m,char}$, should be lower than the residence time for ilmenite particles. It was calculated as the mass of char in the fuel-reactor, $m_{char,FR}$, divided by the char flow that exits the fuel-reactor, sum of the carbon flow from the elutriated char, $C_{char\ elutr}$, and the carbon flow from the char to the air-reactor, $C_{char,AR}$.

$$t_{m,char} = \frac{m_{char,FR}}{C_{char,AR} + C_{char\ elutr}} = \frac{\%C_{char,FR} / 100 \cdot m_{ilm,FR}}{C_{char,AR} + C_{char\ elutr}} \quad (13)$$

$\%C_{char,FR}$ is the carbon concentration from char in the fuel-reactor, which is calculated considering the carbon char flow that exits the fuel-reactor and goes to the air-reactor, $C_{char,AR}$, divided by the sum of the char and ilmenite flows entering the air-reactor.

$$\%C_{char,FR} = \frac{C_{char,AR}}{C_{char,AR} + F_{ilm}} \cdot 100 \quad (14)$$

For the reactivity analysis by TGA, the conversion level of the ilmenite, X_{ilm} , was calculated for the reduction and oxidation reactions as:

$$\text{For reduction: } X_{ilm} = \frac{m_o - m}{R_{O,ilm} \cdot m_o} \quad (15)$$

$$\text{For oxidation: } X_{ilm} = \frac{m - m_r}{R_{O,ilm} \cdot m_o} \quad (16)$$

where m is the instantaneous mass, and m_o and m_r are the mass of fully oxidized and reduced ilmenite at the reacting condition, respectively. The oxygen transport capacity for ilmenite, $R_{O,ilm}$, was defined as the mass fraction of the oxygen-carrier that is used in the oxygen transfer, calculated as:

$$R_{O,ilm} = \frac{m_o - m_r}{m_o} \quad (17)$$

The initial oxygen transport capacity of this ilmenite, $R_{O,ilm}$, was 4.0 wt%, being Fe_2TiO_5 and Fe_2O_3 the oxidized species and FeTiO_3 and Fe_3O_4 the final reduced species in a CLC process.

4. Results and discussion

To determine the behavior of ilmenite as oxygen-carrier during coal combustion, several tests were carried out at different temperatures and for different particle sizes of coal. In addition, to evaluate the volatile matter combustion, as well as the char gasification itself in the continuous testing, experiments with char coal feed were also done. Furthermore, the effect of the oxygen-carrier in gasification and combustion of coal was assessed by carrying out experiments with an inert bed material.

The CLC prototype was easy to operate and control, and the steady state for each operating condition was maintained for at least 30 min. The experiments have been carried out when

ilmenite was already activated for reduction, so that the reactivity of ilmenite was maximum and constant and did not affect the evaluation of other parameters. Nevertheless, the activation process during the first hours of operation will be later analyzed.

As representative of the gas distributions obtained in this study, the evolution with time of temperature and gas concentration from the air and fuel-reactors is shown in Figure 3 for experimental tests with the coal particle size of +125-200 μm for different fuel-reactor temperatures when it was increased from 820 to 950°C. The concentrations in fuel-reactor are in dry basis and N_2 free. Steady state after any parameter change was fast reached and all the points were therefore evaluated at stable conditions. The outlet of the fuel-reactor was mainly composed of oxidized CO_2 , and H_2 and CO as not fully oxidized products of devolatilization and char gasification.

4.1. Effect of the fuel-reactor temperature on the process

The influence of the fuel-reactor temperature on the main parameters of the CLC process for different coal particle sizes was studied. As seen in Figure 3, the outlet of the fuel-reactor is mainly composed of oxidized CO_2 , and H_2 and CO as not fully oxidized products of char gasification. It is remarkable to note that the amount of CH_4 measured in all experiments was low.

Besides, special experiments were carried out at constant conditions for longer than one hour to determine the presence of higher hydrocarbons, tar measurements in the fuel-reactor were done using tar protocol. The results showed that there were no tars in the fuel-reactor outlet flow. Later GC measurements proved also that there were no $\text{C}_2\text{-C}_4$ volatiles in the fuel-reactor. It was therefore considered for the calculations that all hydrocarbons from the pyrolysis of the introduced coal heavier than CH_4 were partially or fully oxidized in the fuel-reactor by ilmenite and came out in the fuel-reactor product gas. On the whole, the product

gas was only composed by CH₄, CO₂, CO, H₂ and H₂O. Furthermore, CH₄ concentration was always below 3% in dry and N₂ free basis.

There was some char elutriation from the fuel-reactor during the experiments. Black solid particles, which were analyzed to be char particles, were recovered in the first liquid container of the tar condensation train. An estimation of the elutriated char flow was done, by filtering, drying and weighting the amount of char that was collected in the mentioned container during one hour of continuous stable operation. The measured elutriated char flow by this method was similar to the elutriated char flow calculated as the difference between the fed coal carbon and the measured carbon in the fuel-reactor and air-reactor outlet gas flows. Thus, the so-called effective coal that was really fed into the system is the sum between the volatile matter and the char flow that was not elutriated.

Figure 4 shows the variation with the temperature of concentrations of CO₂, CO and H₂ at the outlet of the fuel-reactor in dry and free N₂ basis for the different particle sizes. On the one hand, the gasification rate is faster at higher temperatures and higher amount of gasification products are generated. On the other hand, combustion reactions are also promoted with increasing temperatures, and therefore more CO₂ and H₂O as products of combustion are generated. This has a positive effect on the char conversion, because the oxidation of CO and H₂ leads to a lower amount of these gasification inhibitors in the fuel-reactor. The gas composition was similar for coal particle sizes of +125-200 μm and +200-300 μm. However, a lower amount of carbon was detected for the lower particle size (+74-125 μm) because a relevant fraction of char was elutriated from the bed. This issue will be analyzed in the next section.

Figure 5 represents the char conversion and carbon capture and combustion efficiencies as a function of the reactor temperature for different coal particle sizes. As it was presumable, the results show that there is a continuous increase of efficiency with the temperature for all coal

particle sizes. Char conversion changed from 15% at 870°C to 82% at 950°C as extreme cases. For the middle and bigger particle sizes, the combustion efficiency varied from 70% at 870°C to 95% at 950°C. It is likely that the combustion efficiencies observed for the smaller particle size were lower because more char particles are elutriated and do not get in contact with the oxygen-carrier. This is later further discussed. The carbon capture at 870°C had a value of 35% and increased up to 86% at 950°C. The calculated char concentration in the fuel-reactor bed for all the experiments was about 0.35%. If a carbon separation system was implemented, the carbon capture efficiency should be higher, as well as the char concentration in the fuel-reactor should increase until the new steady state was reached.

At the lower temperature the carbon capture efficiency is close to the volatile matter content of the coal, see Table 1. This means that most of carbon in the gases comes from the volatiles, and few amounts of char are being gasified. Note that in this rig and most notably below 920°C, carbon capture presents low values. This is because the gasification rate at these temperatures is slow and thus a relatively high amount of char goes to the air-reactor.

The increase in the carbon capture efficiency with the temperature is due to more carbon in char is being gasified in the reactor. If the trends are extrapolated, it could be expected that all efficiencies would reach a value close to 100% at 1000°C, which means that most of carbon in the coal would exit with the fuel-reactor flue gases. This trend is in concordance with the results found at high temperatures by Berguerand et al. (Berguerand et al., 2009b). At 950°C they obtained carbon capture efficiency of 82-96% for South African coal (Berguerand et al., 2009a) and between 60% and 75% for petroleum coke (Berguerand et al., 2008b).

Figure 6 shows the oxygen demand due to the unburnt gases present in fuel-reactor, Ω_T , at the different temperatures and the coal particle sizes used. Regarding the temperature, it can be seen that Ω_T decreases because of the increase in ilmenite reaction rate with the temperature. However, the Ω_T drop is slight. This can be explained through the raise of the gasification

rate: there is more production of the gasification products, H₂ and CO, which must react with ilmenite. This fact suggests that the increase in the oxygen-carrier reactivity with the temperature is comparable to the increase of the gasification rate. For the medium and bigger coal particle size tested, the oxygen demand was within the values 5-10% for the temperature range 820-950°C. Higher oxygen demand was determined for the smallest particle size.

4.2. Effect of the coal particle size

The effect of the coal particle size on the process performance was investigated because it is a key parameter in the operation of fluidized-bed reactors. As it can be seen in Figure 5, minor differences were found for the char conversion and carbon capture with different particle size. However, a more detailed analysis shows that the oxygen demand depended on the particle size. Figure 6 showed that the total oxygen demand, Ω_T , increased as the particle size was decreasing. This behavior can be related to different flow of char elutriated from the bed for different particle size. Figure 7 shows the calculated fraction of elutriated char for the different experiments made at different temperatures and coal particle sizes. As expected, smaller particles are more easily elutriated than bigger particles. For particle sizes of +74-125 μm about 35% of the introduced char had been elutriated, whereas lower values than 5% were found in most cases for bigger particles.

The lower values calculated for the combustion efficiency or higher oxygen demands for the smaller particles in this unit were related to the relatively high amounts of CO and H₂ in the gas product from fuel-reactor, showed in Figure 4. Unconverted gaseous products, i.e., CO, H₂ and CH₄, can come from a partial oxidation of the gases in the fuel-reactor, as well as char gasification in the fuel-reactor freeboard. The high values obtained for elutriated char with the lower coal particle size caused a higher fraction of char in the freeboard for smaller particles. The result was therefore that gasified fuel particles in the freeboard had not been in contact

with the ilmenite particles that remain at the bottom bed and thus production of CO and H₂, was higher for the smaller coal size. Thus, the combustion efficiency decreased for the particle size of +74-125 μm (see Figure 5) because the gasification products in the freeboard were not burnt, although the char conversion was rather constant. Indeed, the total oxygen demand, Ω_T , increased when the particle size decreased (see Figure 6).

The average mean residence time of ilmenite in the above described experiments was 9 minutes. However, as there was char elutriation, the residence time of char particles should be lower than it was for ilmenite. **Error! Reference source not found.** 8 represents the ratio between the calculated mean residence time of char particles and mean residence time of ilmenite particles for different temperatures and coal particle sizes. Residence times of char, $t_{m,char}$, were always lower than ilmenite residence times, $t_{m,ilm}$. This difference was a consequence of the char elutriation. For the bigger coal particle size the ratio between the residence time of char and ilmenite particles was very close to the unity and the $t_{m,char}/t_{m,ilm}$ ratio was lower for smaller particles because the fraction of elutriated particles was higher. At about 900°C the residence time of char was 9 min for +200-300 μm, 8 min for +125-200 μm and decreased to 5 min for +74-125 μm. Smaller particles had lower time for gasification in the reactor than coarse particles. However, the char conversion is barely affected by the particle size because both the numerator and denominator of Eq. 9 decrease with the coal particle size. The amount of char gasified in the fuel-reactor was therefore lower for smaller particle sizes as well as the effective char introduced. Furthermore, the difference between $t_{m,char}$ and $t_{m,ilm}$ was greater for higher temperatures. This decrease of $t_{m,char}$ with the temperature could be because at higher temperatures char gasification is promoted, being the smaller or more porous resulting char particles easier elutriated.

If a simplified model is used, an approximation to the char gasification rates for the experiments performed at different temperatures with the coal particle sizes tested can be

obtained. The fuel-reactor is considered to follow a continuous stirred-tank reactor (CSTR) model. It is also assumed that the solid fuel reacts at a rate which is proportional to the mass. The carbon char lost exiting the fuel-reactor that enters the air-reactor, $C_{\text{char,AR}}$, can be expressed as a function of the effective carbon char introduced in the CLC system, $C_{\text{char,eff}}$, and $(-r_C) \cdot t_{\text{m,char}}$, where $(-r_C)$ is the rate of char coal conversion and $t_{\text{m,char}}$ is the char mean residence time:

$$\frac{C_{\text{char AR}}}{C_{\text{char eff}}} = \frac{1}{(-r_C) \cdot t_{\text{m,char}} + 1} \quad (18)$$

Figure 9 shows the calculated char gasification rates with this simplified model for experiments performed at a temperature range and for the three particle sizes tested. The gasification rate increased with the temperature for every particle size.

The gasification rates at different temperatures using steam as gasification agent for El Cerrejón coal was obtained also by Linderholm et al. (Linderholm et al., 2010). For a comparison purpose, Figure 9 also represents the theoretical gasification rate as a function of the temperature that would be expected as for these mentioned results. The values for char gasification obtained in this continuous performance are close to the previous results from batch testing by Linderholm et al. (Linderholm et al., 2010), but somewhat lower. However, the gasification rates here obtained were higher than the corresponding found with TGA analysis (Cuadrat et al. 2011d).

As it was stated before with the char conversions, it can be seen that in general the gasification rate does not depend on the particle size, as the values are similar at a given temperature for the coal particle size tested. Nevertheless, for the smaller particle size the values were lower at higher temperatures. This was because for the +74-125 μm particles

there was some gasification taking place in the freeboard and lower gasification rates in the bed were obtained, which is in line with what was already seen.

4.3. Char gasification

10 experiments were done using char coal previously produced in FB fluidized with N₂ in which the temperature in the fuel-reactor was varied from 815 to 910°C. The ultimate analysis of the char is shown in Table 2. The fuel feed was 60.5 g/h, which corresponds to a thermal power of 370 W_{th}. The char particle size used was +125-200 μm. For further comparison, the results obtained are analyzed together with the results of the +125-200 μm coal tests, for which 10 experiments with T_{FR} variation were done.

Figure 10 shows the free N₂ basis CO₂, CO and H₂ dry concentrations obtained in the fuel-reactor at different fuel-reactor temperatures for all experiments tested when feeding +125-200 μm char and when introducing +125-200 μm coal as fuel. The oxidation with ilmenite of the gasification products increases with the temperature, which causes the decrease of CO and H₂ and fast increase in the CO₂ concentration with T_{FR} when using char as fuel. Above 890°C the fuel-reactor exit flow is practically composed only by CO₂ in dry basis. This trend can be also seen in the tests with coal, but smoother, since the combustion behavior of volatile matter is different.

For char as fuel, the carbon capture and the defined char conversion are coincident. The char conversion using char as fuel increased with the temperature from 5% at 820°C to 23% at 910°C. The char residence times were calculated to be 3-5 minutes. As it can be seen in Figure 11, for coal experiments higher char conversions were obtained. This was because the char residence time in these tests was higher: 5-12 min. Higher char fraction was elutriated when using char as fuel, about 25%, whereas for the coal tests used as reference was 10-20%.

The oxygen demand for char particles at temperatures higher than 890°C was equal to zero (see Figure 12), that is, although not all the char was gasified, the produced gases were burnt by ilmenite, which corresponded to a combustion efficiency close to 100% (see Figure 11). This confirmed that the gasification is the limiting step of this process. Since in the large scale the CLC process will be performed at high temperatures and for enough oxygen-carrier bed mass, it is expected that the combustion efficiency of the gasification products reached high values. Thus, the outgoing unburnt gases seen in the fuel-reactor when using coal as fuel were part of the volatile matter that had not been fully oxidized by ilmenite, and the oxygen demand observed at higher temperatures was mainly due to some unburnt volatile matter. In addition, other possible problems that could cause unburnt gases in the fuel-reactor, would be caused by the later gasification of elutriated char particles in the fuel-reactor freeboard that would not be in contact with ilmenite particles, or insufficient residence time in contact with ilmenite of part of the gasification products.

Thus, in order to avoid unreacted fuel gases in offgas a subsequent oxygen polishing step can be implemented, as already proposed by Berguerand et al. (Berguerand, 2008a). To reduce the oxygen requirements in this polishing step, an improved design of the fuel-reactor could be done in order to get better contact between the volatile matter and the oxygen-carrier particles.

4.4. Volatile matter combustion

A key aspect of the process is the oxidation of the gasification products by ilmenite, as well as the released volatile matter, and possible tars formed. In order to evaluate to what extent ilmenite oxidizes the volatile matter, an experiment with sand as inert bed material was done with coal as fuel at 915°C and steam as gasification agent in the fuel-reactor. The total sand bed mass in the system was 1.8 kg and the solid bed mass in the fuel-reactor was 0.38 kg sand.

The results obtained were compared to the experiments performed at the same temperature with ilmenite as bed material with coal as fuel and with char as fuel. GC analysis of the outgoing fuel-reactor gases was done to measure possible hydrocarbons, and possible tar formation was also measured following the tar protocol. The fed coal flow was 75 g/h. The particle size used was +125-200 μm and it is here compared with the test performed at 915°C with +125-200 μm coal and ilmenite as bed material, for which the coal flow was 48 g/h.

For sand as bed material, the GC measurement showed that the fuel-reactor product gas had compositions of 0.13% C_2H_6 and 0.04% C_3H_8 . Besides, the tar content in the fuel-reactor was measured to be 0.895 g/Nm³ dry gas, following the tar protocol. Although the quantities measured of both tars and higher hydrocarbons for this fuel were quite low in absence of an oxygen-carrier, ilmenite has shown to help with the decomposition and later oxidation of those species, since no tars either higher hydrocarbons than CH_4 were formed when using ilmenite.

A summary with the main results of both continuous tests using sand and ilmenite are gathered in Tables 4, 5 and 6. From the ultimate and proximate analysis, the carbon corresponding to the volatile matter, and consequently, the carbon coming from char gasification were calculated. Table 4 shows the fractions from the fuel-reactor product gas that correspond to both volatile matter and gasification products. 88.5% of the carbon contained released gases with sand as bed material came from released volatile matter. But when using ilmenite, the relevance of volatile matter decreased because more gases were released as char was being faster gasified. Table 5 shows the ratio of the carbon containing gases from the volatile matter. For sand as bed material, 36.7% of the carbon from volatile matter exited in form of CO , and 10.2% in form of CH_4 . When using ilmenite, all the CO , CH_4 and H_2 measured came from unburnt released volatile matter, as the tests with coal char showed that the gasification products were fully oxidized. For the tests with ilmenite, some CO was

oxidized and 23.7% of carbon from the volatile matter exited as CO, the CH₄ fraction decreased to 6.3% and the CO₂ fraction increased to 70%. From the comparison between both tests, it turned out that at 915°C the gas conversion of the released volatiles by the reaction with ilmenite was 38.3% for CH₄, 35.3% for CO and 79.0% for H₂. The reaction differences between gases are due to the reaction rates of ilmenite, since it reacts faster with H₂ and slower CH₄ (Abad et al., 2011). In addition, more oxygen transfer is needed to oxidize CH₄. Thus, 63.0% of the oxygen demanded to fully burn the volatile matter fraction was supplied by ilmenite.

Besides, Table 6 shows all the calculated efficiencies and mean residence times for char and the bed material. Char conversion increased from 5.2% to 48.1%. This can be explained through the inhibition effect that causes the presence of high amounts of H₂ and CO in the fuel-reactor, as they do not react with the oxygen-carrier. Obviously, the combustion efficiency was almost zero, as sand is no oxygen-carrier.

4.5. Activation of ilmenite in the continuous rig

Solids samples were extracted during the continuous experiments at several operating times. Since the initial material is calcined ilmenite, an activation process is expected to happen with the number of the red-ox cycles, as it was previously seen from batch experiments (Cuadrat et al., 2011c). A sample taken from the air-reactor after the experiments was analyzed by XRD. Fe₂TiO₅, Fe₂O₃ and TiO₂ were found to be the major components. A semi-quantitative analysis done by XRD showed that the ratio between the weight compositions of the main active species for the oxygen transfer Fe₂TiO₅:Fe₂O₃ of milled particles was 82:18. That is, as for the XRD analysis there were no major changes in the composition of the particles, compared to the composition of the initial material (Adánez et al., 2010). Furthermore,

another sample taken from the fuel-reactor was analyzed by XRD and it was proven to be mainly composed by a mixture of Fe_2TiO_5 , Fe_2O_3 , Fe_3O_4 , FeTiO_3 and TiO_2 ($\text{Fe}_{1.5}\text{Ti}_{0.5}\text{O}_3$).

Reactivity of ilmenite samples taken after 1, 3, 15 and 35 hours of operation was determined by TGA at 900°C with 5% H_2 +40% H_2O mixtures, and afterwards to oxidation conditions in air. Figure 13 shows the conversion, X_{ilm} , vs. time curves obtained for the reduction and oxidation for the different samples. To compare and observe the activation process undergone by ilmenite (Adánez et al., 2010), the reduction and oxidation conversions for calcined and a fully activated ilmenite sample are also represented. The activation undergone by ilmenite with the number of hours can be seen. It can be considered that ilmenite is already active after 3 hours for the reduction reaction, although the reactivity increases further in minor extension after 15 h.

Nevertheless, ilmenite is not completely activated for oxidation reaction after 35 hours operation yet. As it can be seen in Figure 12, the oxidation takes place in two steps and the change to the second phase occurs at higher conversions for samples taken after more hours of operation. Abad et al. (Abad et al., 2011) concluded that the oxidation reaction for ilmenite follows a changing grain size model with two steps, being the first one faster and determined by the chemical reaction control and the second one is slower and controlled by the diffusion in the solid product. That is, an increase in the porosity decreases the relative importance of the second step. Calcined ilmenite had a porosity of 1.2%, after 15 hours the porosity increased to 9.7% and after 35 cycles the measured porosity was 12.3%. The fully activated ilmenite sample is the same shown by Adánez et al. (Adánez et al., 2010) and it was activated after 100 redox cycles in TGA using H_2 as reducing agent, which had a porosity of 35%. The activation process was promoted by high variation of solids conversion in successive redox cycles. The average change in ilmenite conversion in the experiments was low, $\Delta X_{\text{ilm}} = 0.23$, and therefore a higher porosity development and full activation could not happen yet.

Besides, there is one further factor affecting the ilmenite properties during the redox cycles. In a previous work it was observed that ilmenite undergoes a migration phenomenon of the iron oxide present towards the external part of the particle while the core gets titanium enriched. That segregation leads to a gradual decrease in the oxygen transport capacity of the oxygen-carrier (Adánez et al., 2010). The oxygen transport capacity of ilmenite for samples taken at different operation times was determined by TGA and it was seen that it was maintained roughly constant with the operation time. A slight decrease from 4.0% for calcined ilmenite to 3.9% for particles used during 35 h in the unit was observed. In previous work (Cuadrat et al., 2011b) faster decrease in the oxygen transport capacity was measured and need of higher inventories in real CLC continuous systems was foreseen. After undergoing 100 redox cycles in 56 hours with a syngas mixture as reducing agent, the oxygen transport capacity decreased from 4.0 to 2.1%. The oxygen-carrier was however in those experiments further reduced, as X_{ilm} was about 0.65 (considering $R_{O,ilm} = 4.0\%$). Thus, a low value of ΔX_{ilm} allows maintaining the initial $R_{O,ilm}$ roughly constant during long time. In fact, SEM microphotographs of samples extracted from the CLC reactor do not show iron migration towards the outer part of the particle.

5. Conclusions

The capability of ilmenite as oxygen-carrier to burn coal as fuel in a $500W_{th}$ unit has been analyzed by obtaining the carbon capture and combustion efficiencies of the fuel-reactor at a temperature range and with several particle sizes of coal. A bituminous Colombian coal “El Cerrejón” was used as fuel. At higher fuel-reactor temperatures, gasification and combustion reactions are faster and promoted. Carbon capture and combustion efficiencies grow with the temperature, with a faster increase at $T > 910^{\circ}C$. Little CH_4 was measured in all experiments and there were no tars in the fuel-reactor outlet flow. From $870^{\circ}C$ the char conversion was

15% and reached a value of 82% at 950°C. The combustion efficiency varied from 70% at 870°C to 95% at 950°C. Although the carbon capture efficiency in this rig is not representative for the CLC technology, since it does not have a carbon stripper, high carbon capture efficiencies are expected to be obtained, as well as high combustion efficiency, specially at temperatures higher than 950°C. Values for the total oxygen demand from 5% to 15% were found in all the experimental work, mainly due to unconverted CO and H₂. Thus, oxygen polishing need was quite low.

The experiments performed with char coal as fuel confirmed that the gasification is the limiting step of this process. However, the outgoing unburnt gases in the fuel-reactor measured when using coal as fuel, that is, CH₄, CO and H₂, came from volatile matter that had not been fully oxidized by ilmenite.

At 915°C the gas conversion of the released volatiles by the reaction with ilmenite was 38.3% for CH₄, 35.3% for CO and 79.0% for H₂. The reaction differences between gases were due to the reaction rates of ilmenite, since it reacts faster with H₂ and slower CH₄. 63.0% of the oxygen demanded to fully burn volatile matter is supplied by ilmenite. Besides, char gasification was promoted by the presence of the oxygen-carrier, as ilmenite reacts with H₂ and CO, which are gasification inhibitors.

Minor effect on the char conversion can be expected when the coal particle size is varied. However, it is presumable that gasification continues in the fuel-reactor freeboard, this being more relevant for smaller particles. Thus, it is expected that the oxygen demand would increase as the coal particle size decreases.

Activation of ilmenite with the operating time in the unit was observed. For the reduction it can be considered that ilmenite is already active after 3 hours. On the other hand, the oxidation reaction is not fully activated after 35 hours operation yet. A decrease on the oxygen transport capacity of ilmenite was not observed.

Acknowledgments

This work was partially supported by the European Commission, under the RFCS program (ECLAIR Project, Contract RFCP-CT-2008-0008), from Alstom Power Boilers and by the Spanish Ministry of Science and Innovation (Project ENE2010-19550). A. Cuadrat thanks CSIC for the JAE Pre. fellowship. Alberto Abad thanks to the Ministerio de Ciencia e Innovación for the financial support in the course of the I3 Program.

Nomenclature

AR Air-reactor

FR Fuel-reactor

CLC Chemical-Looping Combustion

$C_{\text{char AR}}$ carbon flow from the char that goes to the air-reactor (mol/s)

$C_{\text{char FR}}$ carbon flow from the gasified char in the fuel-reactor (mol/s)

$C_{\text{char eff}}$ carbon flow from the effective char introduced (mol/s)

$C_{\text{char elutr}}$ carbon flow from the elutriated char (mol/s)

C_{FR} outlet carbon flow from the fuel-reactor (mol/s)

C_{vol} carbon flow coming from the volatile matter fed (mol/s)

F_{AR} outlet air-reactor gas flow (mol/s)

$F_{\text{CH}_4,\text{FR}}, F_{\text{H}_2,\text{FR}}, F_{\text{CO},\text{FR}}, F_{\text{CO}_2,\text{FR}}, F_{\text{H}_2\text{O},\text{FR out}}$ outlet flows in the fuel-reactor of CH_4 , H_2 , CO , CO_2 and H_2O , respectively (mol/s)

$F_{\text{CO}_2,\text{AR}}$ outlet flow in the air-reactor of CO_2 (mol/s)

F_{FR} dry basis product gas flow (mol/s)

$F_{\text{H}_2\text{O},\text{in}}$ water steam inlet flow in the fuel-reactor (mol/s)

F_{ilm} solids circulation rate (kg/s)

$F_{\text{N}_2,\text{AR}}$ N_2 inlet flow in the fuel-reactor (mol/s)

$F_{\text{N}_2,\text{FR}}$ N_2 inlet flow in the fuel-reactor (mol/s)

Me_xO_y oxidized oxygen-carrier

$\text{Me}_x\text{O}_{y-1}$ reduced oxygen-carrier

$m_{\text{char,FR}}$ mass of char in the fuel-reactor (kg)

$m_{\text{ilm,FR}}$ fuel-reactor bed mass or solid hold-up in the fuel-reactor (kg)

m instantaneous mass of the oxygen-carrier (kg)

m_r mass of the reduced form of the oxygen-carrier (kg)

m_o mass of the oxidized form of the oxygen-carrier (kg)

O_2 demand coal,eff oxygen demand of the effective coal fed (moles O_2/s)

$(-r_C)$ rate of char coal conversion (s^{-1})

$R_{O,ilm}$ oxygen transport capacity of ilmenite

T_{FR} temperature in the fuel-reactor ($^{\circ}C$)

X_{char} char conversion

X_{ilm} reaction conversion of ilmenite

$y_{O_2,AR}$, $y_{CO_2,AR}$ fractions in the air-reactor outlet flow of O_2 and CO_2

$y_{CH_4,FR}$, $y_{CO_2,FR}$, $y_{CO,FR}$, $y_{H_2,FR}$ dry basis fractions in the fuel-reactor product gas of CH_4 , CO_2 , CO , H_2 , respectively

ΔX_{ilm} variation of reaction conversion of ilmenite

η_{CC} carbon capture efficiency

η_{comb} combustion efficiency

$t_{m,char}$ mean residence time of char (s)

$t_{m,ilm}$ mean residence time of ilmenite (s)

Ω_T total oxygen demand of fuel-reactor product gas

$\%C_{char,FR}$ char concentration in the fuel-reactor (%)

REFERENCES

- Abad, A., Adánez, J., Cuadrat, A., García-Labiano, F., Gayán, P., de Diego, L.F., **2011**. Reaction kinetics of ilmenite for Chemical-looping Combustion. *Chemical Engineering Science*, 66(4), 689-702.
- Adánez, J., de Diego, L.F., García-Labiano, F., Gayán, P., Abad, A., Palacios, J.M., **2004**. Selection of oxygen-carriers for chemical-looping combustion. *Energy & Fuels*, 18, 371-377.
- Adánez, J., Cuadrat, A., Abad, A., Gayán, P., de Diego, L.F., García-Labiano, F., **2010**. Ilmenite Activation during Consecutive Redox Cycles in Chemical-Looping Combustion. *Energy & Fuels*, 24, 1402-1413.
- Adánez, J., Abad, A., García-Labiano, F., Gayán, P., de Diego, L.F., **2011**. Chemical-Looping Technologies: a Review. *Submitted for publication*.
- Berguerand, N., Lyngfelt, A., **2008a**. Design and operation of a 10 kWth chemical-looping combustor for solid fuels – Testing with South African coal. *Fuel*, 87, 2713-2726.
- Berguerand, N.; Lyngfelt, A., **2008b**. The Use of Petroleum Coke as Fuel in a 10 kWth Chemical-Looping Combustor. *International Journal of Greenhouse Gas Control*, 2, 169-179.
- Berguerand, N., Lyngfelt, A., **2009a**. Operation in a 10 kWth chemical-looping combustor for solid fuel—Testing with a Mexican petroleum coke. GHGT-9. *Energy Procedia*, 1(1), 407-414.
- Berguerand, N., Lyngfelt, A., **2009b**. Chemical-looping combustion of petroleum coke using ilmenite in a 10 kWth unit-high-temperature operation. *Energy & Fuels*, 23(10), 5257-5268.

- Bidwe, A.R., Mayer, F., Hawthorne, C., Charitos, A., Schuster, A., Scheffknecht, G., **2010**. Use of ilmenite as an oxygen-carrier in chemical looping combustion-batch and continuous dual fluidized bed investigation. Proc 10th Int Conf Greenhouse Gas Technology (GHGT-10). Amsterdam, The Netherlands (*expected to be published in Energy Procedia*).
- Cao, Y., Pan, W.P., **2006**. Investigation of Chemical Looping Combustion by Solid Fuels. 1. Process Analysis. *Energy & Fuels*, 20, 1836-1844.
- Cuadrat, A., Abad, A., Adánez, J., de Diego, L.F., García-Labiano, F., Gayán, P. **2011a**. Design Considerations for Chemical-Looping Combustion of coal – Part 1. Experimental Tests. *Submitted for publication*.
- Cuadrat, A., Abad, A., Adánez, J., de Diego, L.F., García-Labiano, F., Gayán, P., **2011b**. Behaviour of Ilmenite as Oxygen Carrier in Chemical-Looping Combustion. *Submitted for publication*.
- Cuadrat, A., Abad, A., García-Labiano, F., Gayán, P., de Diego, L.F., Adánez, J., **2011c**. Effect of operating conditions in Chemical-Looping Combustion of coal in a 500 Wth unit. *Submitted for publication*.
- Cuadrat, A., Abad, A., Gayán, P., de Diego, L.F., García-Labiano, F., Adánez, J. **2011d**. Modeling and optimization of Chemical Looping Combustion for solid fuels with ilmenite as oxygen carrier. International Conference on Coal Science & Technology (ICCS&T), October 2011.
- Eide, L.I., Anheden, M., Lyngfelt, A., Abanades, C., Younes, M., Clodic, D., **2005**. Novel Capture Processes. *Oil Gas Science Tech*, 60, 497–508.
- Fossdal, A., Bakken, E., Øye, B.A., Schøning, C., Kaus, I., Mokkelbost, T., Larring, Y., **2010**. Study of inexpensive oxygen carriers for chemical looping combustion. *Int J Greenhouse Gas Control*. doi:10.1016/j.ijggc.2010.08.001.

- Gu, H.M., Wu, J.H., Hao, J.G., Shen, L. H., Xiao, J., **2010**. Experiments on chemical looping combustion of coal in interconnected fluidized bed using hematite as oxygen-carrier. *Proceedings of the Chinese Society of Electrical Engineering*, 30(17), 51-56.
- Hossain, M.M., de Lasa, H.I. **2008**. Chemical-Looping Combustion (CLC) for Inherent. CO₂ Separation - a Review. *Chem Eng Sci*, 63(18), 4433-4451.
- Intergovernmental Panel of Climate Change, **2005**. Special report on carbon dioxide capture and storage, Cambridge University Press, Cambridge, UK (available at www.ipcc.ch).
- Intergovernmental Panel of Climate Change, **2007**. In: Solomon S, Qin D, Manning M, Marquis M, Averyt K, Tignor MMB, et al., editors. The physical science basis. Working group I contribution to the fourth assessment report of the international panel on climate change. Cambridge, United Kingdom, New York, NY, USA: Cambridge University Press.
- Kerr, H.R., **2005**. Capture and separation technologies gaps and priority research needs; in: Thomas, D., Benson, S. (Eds.), Carbon Dioxide Capture for Storage in Deep Geologic Formations—Results from the CO₂ Capture Project; Elsevier Ltd.: Oxford, UK, 1(38).
- Leion, H., Lyngfelt, A., Johansson, M., Jerndal, E., Mattisson, T., **2008a**. The use of ilmenite as an oxygen-carrier in chemical-looping combustion. *Chemical Engineering Research and Design*, 86, 1017-1026.
- Leion, H.; Mattisson, T.; Lyngfelt, A., **2008b**. Solid fuels in chemical-looping combustion. *International Journal of Greenhouse Gas Control*, 2008, 2 (2), 180-193.
- Leion, H., Mattisson, T., Lyngfelt A., **2009**. Use of ores and industrial products as oxygen carriers in chemical-looping combustion. *Energy & Fuels*, 23, 2307-2315.
- Linderholm, C., Cuadrat, A., Lyngfelt, A., **2010**. Chemical-looping combustion of solid fuels in a 10 kWth pilot – batch tests with five fuels. GHGT-10, Amsterdam, 19-23 September 2010 (*expected to be published in Energy Procedia*).

- Markström, P., Berguerand, N., Lyngfelt A., **2010**. The application of a multistage-bed model for residence-time analysis in chemical-looping combustion of solid fuel. *Chem Eng Sci*, 65, 5055-5066.
- Ortiz, M., Gayán, P., de Diego, L.F., García-Labiano, F., Abad, A., Pans, M.A., Adánez, J., **2010**. Hydrogen production with CO₂ capture by coupling steam reforming of methane and chemical-looping combustion: Use of an iron-based waste product as oxygen-carrier burning a PSA tail gas. *Journal of Power Sources*, 196(9), 4370-4381.
- Pröll, T., Mayer, K., Bolhàr-Nordenkamp, J., Kolbitsch, P., Mattisson, T., Lyngfelt, A., Hofbauer, H., **2009**. Natural minerals as oxygen-carriers for chemical looping combustion in a dual circulating fluidized bed system. *Energy Procedia*, 1, 27-34.
- Shen, L., Wu, J., Xiao, J., **2009a**. Experiments on chemical looping combustion of coal with a NiO based oxygen-carrier. *Combustion and Flame*, 156 (3), 721-728.
- Shen, L., Wu, J., Gao, Z., Xiao, J., **2009b**. Reactivity deterioration of NiO/Al₂O₃ oxygen-carrier for chemical looping combustion of coal in a 10 kWth reactor. *Combustion and Flame*,; 156 (7), 1377-1385.
- Shen, L., Wu, J., Gao, Z., Xiao, J., **2010**. Characterization of chemical looping combustion of coal in a 1 kWth reactor with a nickel-based oxygen-carrier. *Combustion and Flame*, 157(5), 934-942.
- Simell, P., Stahlberg, P., Kurkela E., Albretch J., Deutch S., Sjostrom K., **2000**. Provisional protocol for the sampling and analysis of tar and particulates in the gas from large-scale biomass gasifiers. Version 1998. *Biomass and Bioenergy*, 18, 19-38.
- Song, Q., Xiao, R., Deng, Z., Shen, L., Xiao, J., Zhang, M., **2008**. Effect of temperature on reduction of CaSO₄ of simulated coal gas in a fluidized bed reactor. *Ind Eng Chem Res*, 47, 8148-8159.
- Wang, J., Anthony, E.J., **2008**. Clean combustion of solid fuels. *Appl Energy*, 85, 73-79.

The use of ilmenite as oxygen-carrier in a 500 Wth Chemical Looping Coal Combustion unit
A. Cuadrat, A. Abad*, F. García-Labiano, P. Gayán, L. F. de Diego, J. Adánez

Tables

Table 1. Fresh and calcined ilmenite compositions (wt.%).

Table 2. Properties of the used pre-treated Colombian coal.

Table 3. Ultimate analysis of the used pre-treated Colombian char coal.

Table 4. Relative fraction of the carbon from volatile matter and carbon from gasified char in comparison to the total carbon outgoing with the fuel-reactor product gas. Tests with sand and ilmenite as bed material. $T_{FR} = 915^{\circ}\text{C}$.

Table 5. Flows of the generated gases, i.e. CH_4 , CO and CO_2 , released from the devolatilization in comparison to the total carbon contained in the fed volatile matter. Tests with sand and ilmenite as bed material. $T_{FR} = 915^{\circ}\text{C}$.

Table 6. Efficiencies and mean residence times for char and the bed materials: sand and ilmenite. Tests with sand and ilmenite as bed material. $T_{FR} = 915^{\circ}\text{C}$.

Table 1. Fresh and calcined ilmenite compositions (wt.%).

| | Fresh ilmenite | Calcined ilmenite |
|----------------------------------|----------------|-------------------|
| Fe ₂ O ₃ | 14.8 | 11.2 |
| FeTiO ₃ | 65.5 | - |
| Fe ₂ TiO ₅ | - | 54.7 |
| TiO ₂ | 14.0 | 28.6 |
| inerts | 5.7 | 5.5 |

Table 2. Properties of the used pre-treated Colombian coal.

| Fresh Colombian coal | | | |
|--------------------------------|--------|-----------------|--------|
| C | 68.0 % | Moisture | 6.2 % |
| H | 4.2 % | Volatile matter | 33.4 % |
| N | 1.6 % | Fixed carbon | 48.5 % |
| S | 0.6 % | Ash | 11.9 % |
| O | 7.5 % | | |
| Low Heating Value: 25878 kJ/kg | | | |
| Pre-treated Colombian coal | | | |
| C | 65.8 % | Moisture | 2.3 % |
| H | 3.3 % | Volatile matter | 33.0 % |
| N | 1.6 % | Fixed carbon | 55.9 % |
| S | 0.6 % | Ash | 8.8 % |
| O | 17.6 % | | |
| Low Heating Value: 21899 kJ/kg | | | |

Table 3. Ultimate analysis of the used pre-treated Colombian char coal.

| | |
|---|--------|
| C | 79.8 % |
| H | 0.7 % |
| N | 1.3 % |
| S | 0.6 % |
| O | 4.0 % |

Table 4. Relative fraction of the carbon from volatile matter and carbon from gasified char in comparison to the total carbon outgoing with the fuel-reactor product gas. Tests with sand and ilmenite as bed material. $T_{FR} = 915^{\circ}\text{C}$.

| | Coal+Sand | Coal+Ilmenite |
|---|-----------|---------------|
| $\frac{C_{\text{vol}}}{(F_{\text{CH}_4} + F_{\text{CO}} + F_{\text{CO}_2})}$ | 88.5% | 42.6% |
| $\frac{C_{\text{gasif char}}}{(F_{\text{CH}_4} + F_{\text{CO}} + F_{\text{CO}_2})}$ | 11.5% | 57.4% |

Table 5. Flows of the generated gases, i.e. CH₄, CO and CO₂, released from the devolatilization in comparison to the total carbon contained in the fed volatile matter. Tests with sand and ilmenite as bed material. T_{FR} = 915°C.

| | Coal+Sand | Coal+Ilmenite |
|---|-----------|---------------|
| $\left(\frac{F_{\text{CH}_4,\text{FR}}}{C_{\text{FR}}}\right)_{\text{vol}}$ | 10.2% | 6.3% |
| $\left(\frac{F_{\text{CO},\text{FR}}}{C_{\text{FR}}}\right)_{\text{vol}}$ | 36.7% | 23.7% |
| $\left(\frac{F_{\text{CO}_2,\text{FR}}}{C_{\text{FR}}}\right)_{\text{vol}}$ | 53.1% | 70.0% |

Table 6. Efficiencies and mean residence times for char and the bed materials: sand and ilmenite. Tests with sand and ilmenite as bed material. $T_{FR} = 915^{\circ}\text{C}$.

| | X_{char} | η_{CC} | η_{comb} | $t_{\text{m, char}}$ | $t_{\text{m, bed material}}$ |
|---------------|-------------------|--------------------|----------------------|----------------------|------------------------------|
| Coal+Sand | 0.052 | 0.322 | 0 | 6.2 min | 9.4 min |
| Coal+Ilmenite | 0.481 | 0.617 | 0.810 | 5.7 min | 9 min |

The use of ilmenite as oxygen-carrier in a 500 Wth Chemical Looping Coal Combustion unit
A. Cuadrat, A. Abad*, F. García-Labiano, P. Gayán, L. F. de Diego, J. Adánez

Figure captions

Figure 1. Reactor scheme of the CLC with solid fuels process using solid fuels. (--- optional stream)

Figure 2. Schematic diagram of the ICB-CSIC-s1 facility for coal-fuelled CLC.

Figure 3. Gas distributions in fuel-reactor (dry basis and N₂ free concentrations) and air-reactor for increasing fuel-reactor temperature. Solids circulation flow: 3.5 kg/h. Coal particle size: +125-200 μm.

Figure 4. CO₂, CO and H₂ concentration in the fuel-reactor (dry free N₂ basis) at different fuel-reactor temperatures for different coal particle size. Particle size: ○ 74-125 μm; △ 125-200 μm; □ 200-300 μm.

Figure 5. a) Char conversion, b) carbon capture and c) combustion efficiency variation with fuel-reactor temperature for various coal particle sizes. Particle size: ○ 74-125 μm; △ 125-200 μm; □ 200-300 μm.

Figure 6. Oxygen demand variation with the fuel-reactor temperature for different coal particle sizes.

Figure 7. Elutriated char fraction variation with the fuel-reactor temperature for different coal particle sizes.

Figure 8. Ratio between char and ilmenite mean residence times at different fuel-reactor temperatures and for different coal particle sizes. $t_{m,ilm} = 14$ minutes.

Figure 9. Calculated gasification rate considering the fuel-reactor as a CSTR for different fuel-reactor temperatures. Coal particle size: ○ 74-125 μm; △ 125-200 μm; □ 200-300 μm. — Theoretical gasification rate as for the results by Linderholm et al. (Linderholm et al., 2010).

The use of ilmenite as oxygen-carrier in a 500 Wth Chemical Looping Coal Combustion unit
A. Cuadrat, A. Abad*, F. García-Labiano, P. Gayán, L. F. de Diego, J. Adánez

Figure 10. CO₂, CO and H₂ concentration in the fuel-reactor (dry free N₂ basis) at different fuel-reactor temperatures for +125-200 μm char (filled symbol plots) and +125-200 μm coal (void symbol plots).

Figure 11. Char conversion and combustion efficiencies at different fuel-reactor temperatures for +125-200 μm char (filled symbol plots) and +125-200 μm coal (void symbol plots).

Figure 12. Oxygen demand at different fuel-reactor temperatures for +125-200 μm char (filled symbol plots) and +125-200 μm coal (void symbol plots).

Figure 13. Ilmenite conversion vs. time for a) reduction and b) oxidation for calcined ilmenite and for ilmenite samples after 1, 3, 15 and 35 hours of continuous operation. Comparison with the reduction and oxidation conversions of calcined ilmenite (---) and a fully activated ilmenite sample (-·-·-).

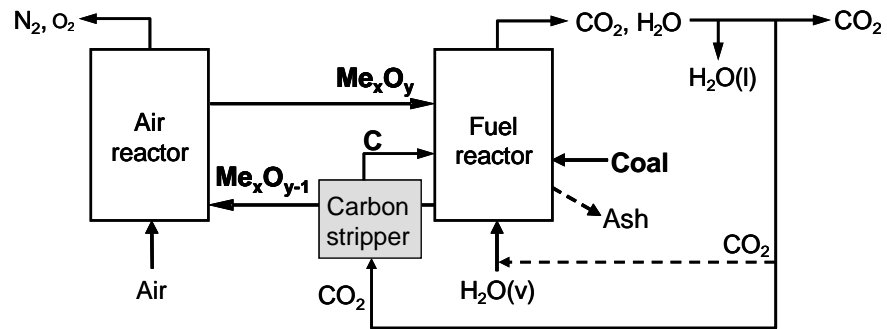


Figure 1. Reactor scheme of the CLC with solid fuels process using solid fuels. (--- optional stream)

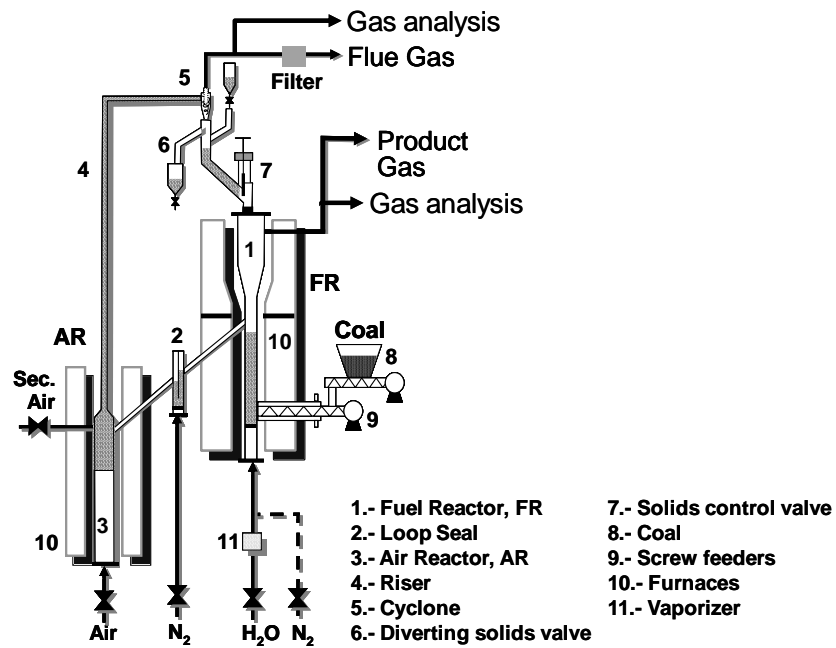


Figure 2. Schematic diagram of the ICB-CSIC-s1 facility for coal-fuelled CLC.

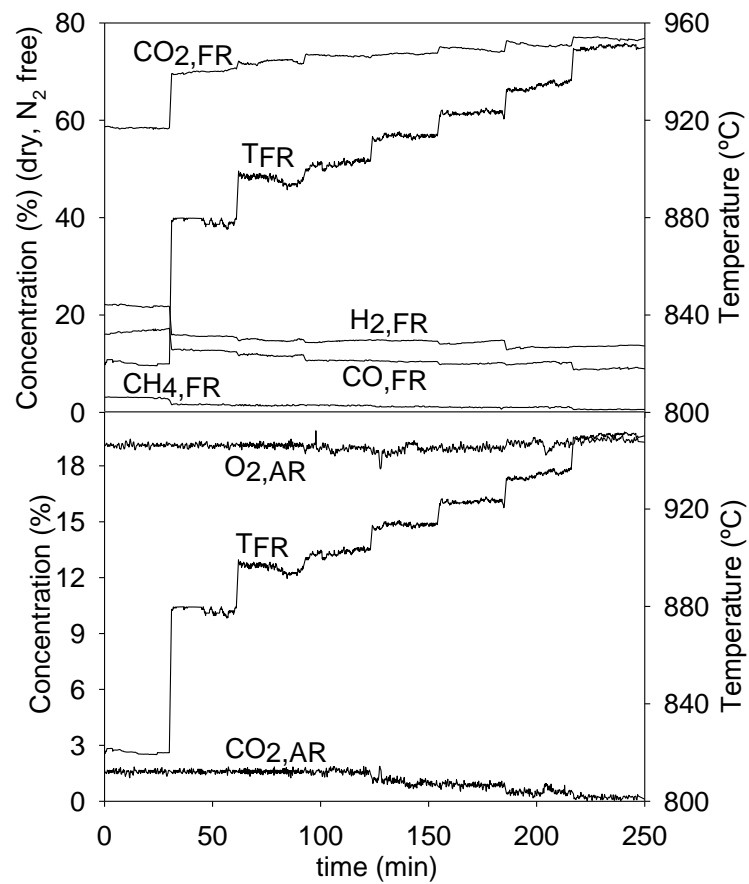


Figure 3. Gas distributions in fuel-reactor (dry basis and N₂ free concentrations) and air-reactor for increasing fuel-reactor temperature. Solids circulation flow: 3.5 kg/h. Coal particle size: +125-200 μm .

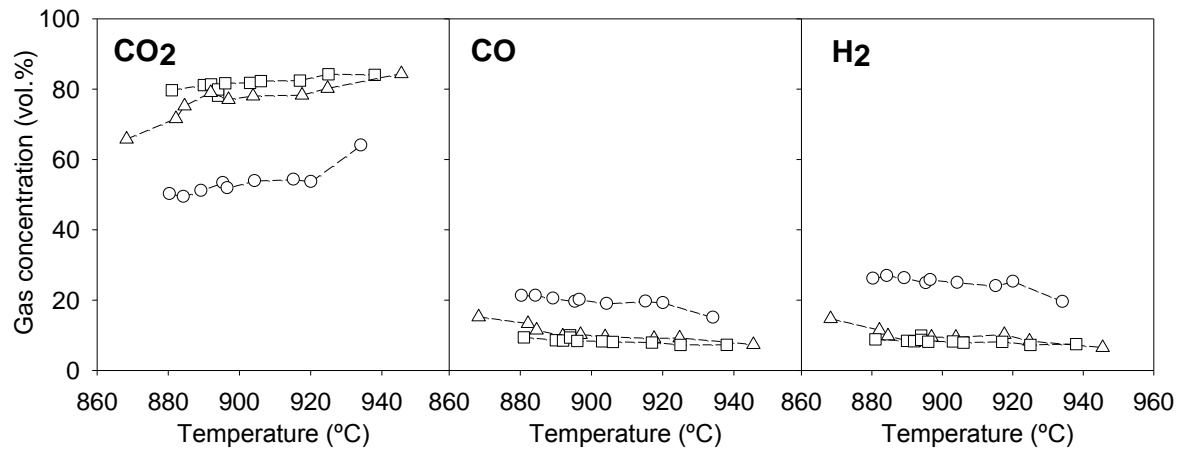


Figure 4. CO₂, CO and H₂ concentration in the fuel-reactor (dry free N₂ basis) at different fuel-reactor temperatures for different coal particle size. Particle size: -○- 74-125 μm; -△- 125-200 μm; -□- 200-300 μm.

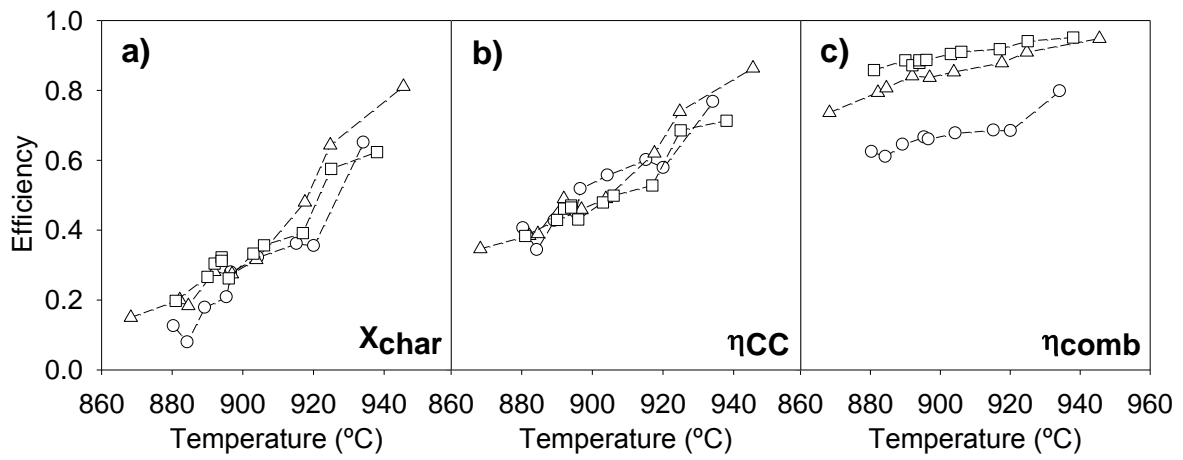


Figure 5. a) Char conversion, b) carbon capture and c) combustion efficiency variation with fuel-reactor temperature for various coal particle sizes. Particle size: \circ 74-125 μm ; \triangle 125-200 μm ; \square 200-300 μm .

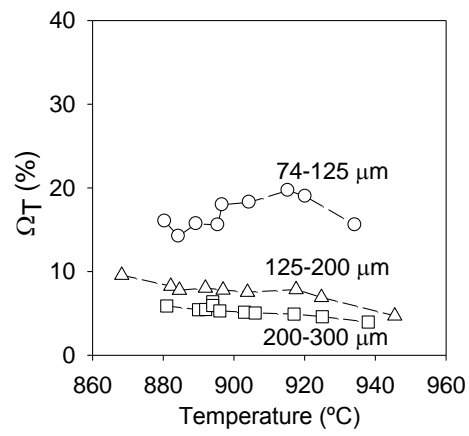


Figure 6. Oxygen demand variation with the fuel-reactor temperature for different coal particle sizes.

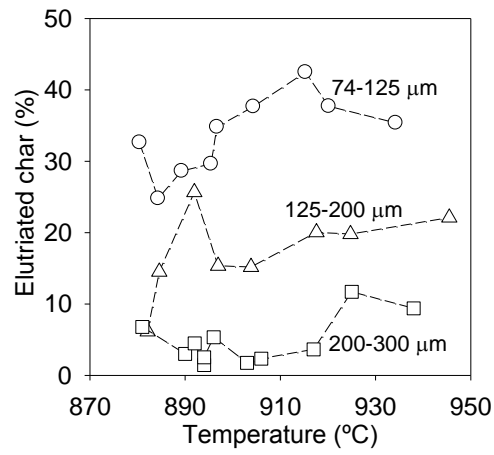


Figure 7. Elutriated char fraction variation with the fuel-reactor temperature for different coal particle sizes.

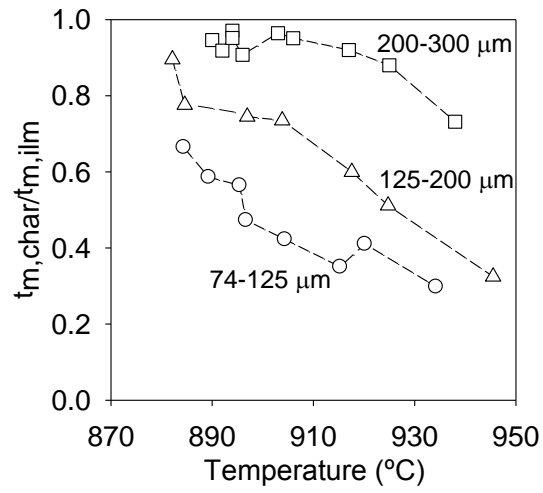


Figure 8. Ratio between char and ilmenite mean residence times at different fuel-reactor temperatures and for different coal particle sizes. $t_{m,ilm} = 14$ minutes.

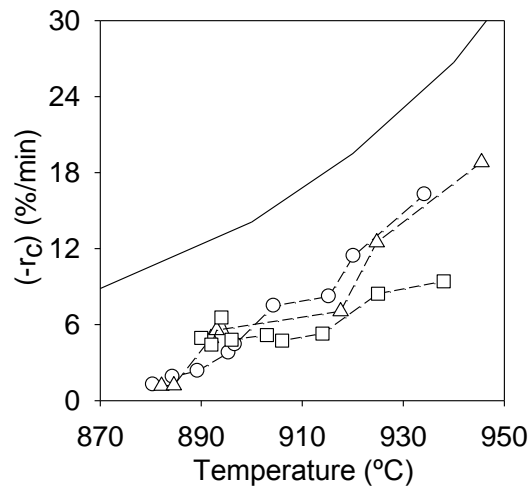


Figure 9. Calculated gasification rate considering the fuel-reactor as a CSTR for different fuel-reactor temperatures. Coal particle size: \circ 74-125 μm ; \triangle 125-200 μm ; \square 200-300 μm . — Theoretical gasification rate as for the results by Linderholm et al. (Linderholm et al., 2010).

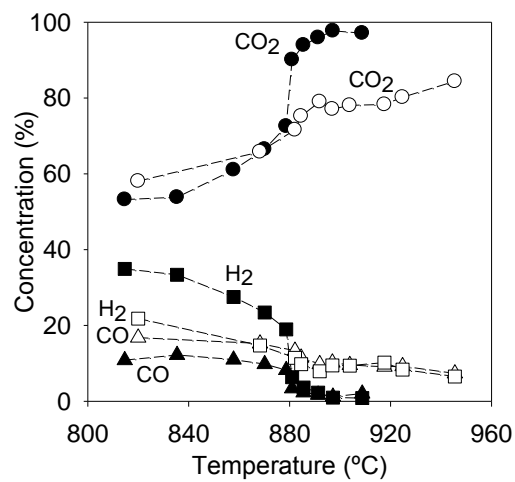


Figure 10. CO₂, CO and H₂ concentration in the fuel-reactor (dry free N₂ basis) at different fuel-reactor temperatures for +125-200 μm char (filled symbol plots) and +125-200 μm coal (void symbol plots).

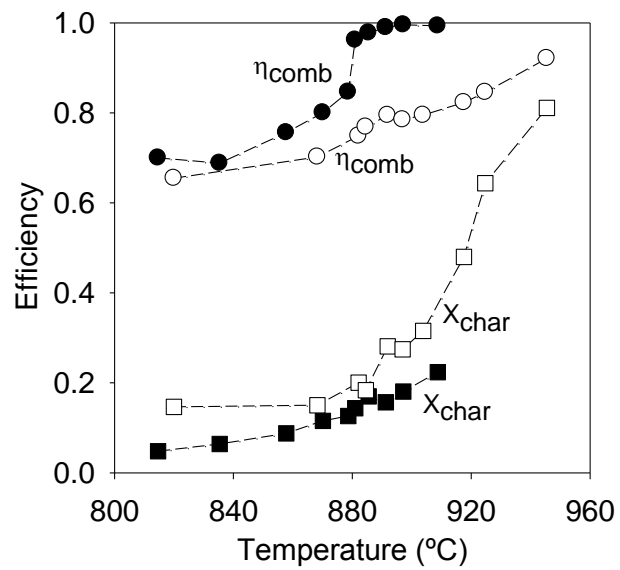


Figure 11. Char conversion and combustion efficiencies at different fuel-reactor temperatures for +125-200 μm char (filled symbol plots) and +125-200 μm coal (void symbol plots).

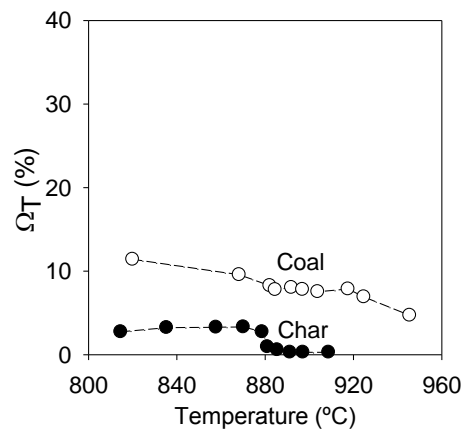


Figure 12. Oxygen demand at different fuel-reactor temperatures for +125-200 μm char (filled symbol plots) and +125-200 μm coal (void symbol plots).

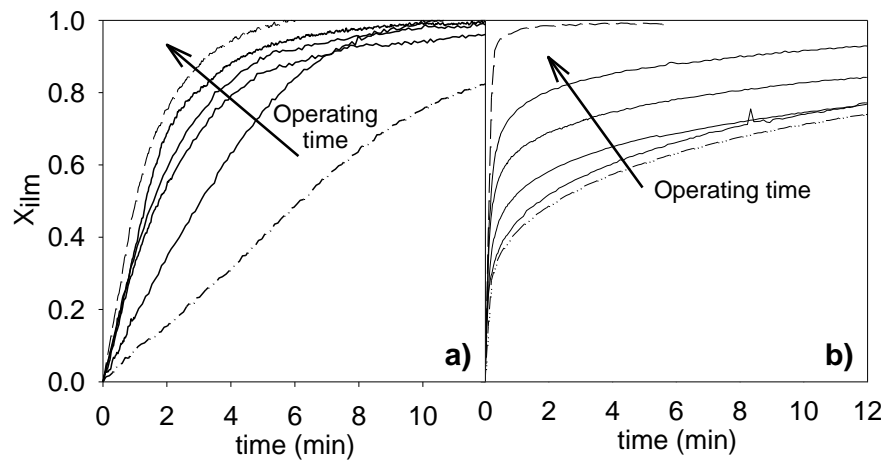


Figure 13. Ilmenite conversion vs. time for a) reduction and b) oxidation for calcined ilmenite and for ilmenite samples after 1, 3, 15 and 35 hours of continuous operation. Comparison with the reduction and oxidation conversions of calcined ilmenite (---) and a fully activated ilmenite sample (-.-.-).